Twin-Related Branching of Solution-Grown ZnSe Nanowires

Dayne D. Fanfair and Brian A. Korgel*

Department of Chemical Engineering, Texas Materials Institute, Center for Nano- and Molecular Science and Technology, The University of Texas at Austin, Austin, Texas 78712-1062

Received May 28, 2007. Revised Manuscript Received July 22, 2007

ZnSe nanowires were grown by the solution−liquid−solid mechanism at 350 °C in either trioctylamine (TOA) or trioctylphosphine oxide (TOPO) using bismuth nanocrystals as seeds. Approximately half of the nanowires produced in TOA had short ZnSe branches off their sidewall surfaces, whereas nanowires grown in TOPO did not exhibit branching. The ZnSe nanowires with branching grew predominantly in the <112> direction with a large number of {111} twins extending down their length. The branches grew epitaxially from the sidewall surface in the <111> direction with a large concentration of lamellar {111} twins. The absence of sidewall nucleation and branching from ZnSe nanowires grown in TOPO can be explained by the stronger surface passivation from TOPO relative to that of TOA.

Introduction

Semiconductor nanowires are promising nanoscale building blocks for new technologies.[1] Nanowires have extremely high aspect ratios (>1000) and surface area-to-volume ratios and can be produced with nanoscale diameters with size-tunable properties resulting from quantum confinement effects.[2] The anisotropic structure of the nanowires, along with their lack of grain boundaries, might facilitate efficient charge (i.e., electrons, holes, excitons) and spin transport over relatively long distances; and furthermore, they can be dispersed in various solvents, making it possible to manipulate them at room temperature for integration with organic materials and flexible substrates.[3,4] Nanowires with increasingly complex geometrical structure, such as branched nanowires,[5] could provide additional tunability of material properties and further increases in the surface area-to-volume ratio, which might be useful in chemical sensing applications, for example, that rely on the surface adsorption of various analytes for detection.

Branching has been observed in nanowires grown via the solution−liquid−solid (SLS) mechanism (such as PbSe, CdSe, and CdTe nanowires seeded by Au/Bi core/shell particles),[6−8] the vapor−solid growth mechanism (such as ZnO nanobelts and nanowires,[9,10] MgO nanowires,[10,11] ZnS nanostructures,[12] and $Zn_xCd_{1-x}Se$ nanocombs[13]), and the vapor−liquid−solid (VLS) growth mechanism (CdSe,[14,15] ZnS (seeded by Au particles),[16] and CdS (seeded by Sn particles)[17]). Branched growth has also been intentionally induced by depositing seed metal particles on the nanowire sidewall surfaces after their synthesis, followed with a second VLS growth step. This process has been demonstrated for branched GaP,[18] Si (seeded by Au particles),[5] GaN (seeded by Ni particles),[5] and InAs nanowires (seeded by Au particles followed by Mn seed particles).[19] Although branching has been observed in these various systems, the factors that limit or encourage branching off nanowire surfaces are not well understood. Herein, we report the SLS growth of ZnSe nanowires seeded by Bi nanocrystals and find that the solvent plays an influential role in branch nucleation and growth off the nanowire surfaces.

ZnSe is a wide band gap (2.7 eV) semiconductor, which makes ZnSe nanowires suitable for applications such as blue/green optoelectronic devices.[20] ZnSe nanowires have been

* Corresponding author. E-mail: korgel@che.utexas.edu. Tel: (512) 471-5633. Fax: (512) 471-7060.

(1) Korgel, B. A.; Hanrath, T.; Davidson, F. M. In *Encyclopedia of Chemical Processing*; Lee, S. K. B., Ed.; Marcel Dekker: New York, 2006; Vol. 1, pp 3191−3203.
(2) Wang, F.; Dong, A.; Sun, J.; Tang, R.; Yu, H.; Buhro, W. E. *Inorg. Chem.* **2006**, *45*, 7511.
(3) Duan, X. F.; Niu, C. M.; Sahi, V.; Chem, J.; Parce, J. W.; Empedocles, S.; Goldman, J. L. *Nature* **2003**, *425*, 274−278.
(4) McAlpine, M. C.; Friedman, R. S.; Lieber, C. M. *Proc. IEEE* **2005**, *93*, 1357−1363.
(5) Wang, D.; Qian, F.; Yang, C.; Zhong, Z. H.; Lieber, C. M. *Nano Lett.* **2004**, *4*, 871−874.
(6) Hull, K. L.; Grebinski, J. W.; Kosel, T. H.; Kuno, M. *Chem. Mater.* **2005**, *17*, 4416−4425.
(7) Grebinski, J. W.; Hull, K. L.; Zhang, J.; Kosel, T. H.; Kuno, M. *Chem. Mater.* **2004**, *16*, 5260−5272.
(8) Kuno, M.; Ahmad, O.; Protasenko, V.; Bacinello, D.; Kosel, T. H. *Chem. Mater.* **2006**, *18*, 5722−5732.
(9) Wei, Q.; Meng, G.; An, X.; Hao, Y.; Zhang, L. *Nanotechnology* **2005**, *16*, 2561−2566.
(10) Lao, J. Y.; Huang, J. Y.; Wang, D. Z.; Ren, Z. F. *J. Mater. Chem.* **2004**, *14*, 770−773.
(11) Hao, Y.; Meng, G.; Ye, C.; Zhang, X.; Zhang, L. *J. Phys. Chem. B* **2005**, *109*, 11204−11208.
(12) Moore, D.; Wang, Z. L. *J. Mater. Chem.* **2006**, *16*, 3898−3905.
(13) Zhai, T.; Zhang, X.; Yang, W.; Ma, Y.; Wang, J.; Gu, Z.; Yu, D.; Yang, H.; Yao, J. *Chem. Phys. Lett.* **2006**, *427*, 371−374.
(14) Wang, G. X.; Park, M. S.; Liu, H. K.; Wexler, D.; Chen, J. *Appl. Phys. Lett.* **2006**, *88*, 193115.
(15) Ding, Y.; Ma, C.; Wang, Z. L. *Adv. Mater.* **2004**, *16*, 1740−1743.
(16) Moore, D.; Ding, Y.; Wang, Z. L. *Angew. Chem., Int. Ed.* **2006**, *45*, 5150−5154.
(17) Zhang, J.; Yang, Y.; Jiang, F.; Li, J.; Xu, B.; Wang, S.; Wang, X. *J. Cryst. Growth* **2006**, *293*, 236−241.
(18) Dick, K. A.; Deppert, K.; Larsson, M. W.; Martensson, T.; Seifert, W.; Wallenberg, L. R.; Samuelson, L. *Nat. Mater.* **2004**, *3*, 380−384.
(19) May, S. J.; Zheng, J.-G.; Wessels, B. W.; Lauhon, L. J. *Adv. Mater.* **2005**, *17*, 598−602.
(20) Hines, M. A.; Guyot-Sionnest, P. *J. Phys. Chem. B* **1998**, *102*, 3655−3657.

10.1021/cm071440t CCC: $37.00
Published on Web 09/11/2007

produced by vapor-phase[21−32] and solution-phase[33−37] routes. Furthermore, branched ZnSe structures have been observed by Yao et al. (branched sub-micrometer ZnSe wires)[38] and Golberg et al. (branched ZnSe nanorods).[39] Here, we show that the solvent used for the SLS growth process is very important—nanowires grown in trioctylphosphine oxide (TOPO) do not exhibit branching, whereas nanowires grown in trioctylamine (TOA) have significant nanowire sidewall branching. Additionally, twinning in the nanowires appears to be intimately involved in branch growth, promoting <112>-oriented nanowire growth that subsequently exposes reactive {111} sidewall surfaces that seed the growth of the branches.

Experimental Details

Materials. Tri-*n*-octylphosphine (97%, TOP), TOPO (99%), bismuth (III) 2-ethylhexanoate, and selenium powder were used as received from Strem. Zinc oxide (99.999%), oleic acid (≥60%, OA), ethylenediamine, dioctylether (≥90%), sodium borohydride, and TOA (98%) were used as received from Sigma-Aldrich, and all other solvents were used as received from Fisher Scientific without further purification. For all nanowire growth reactions, a reagent solution of 1 M elemental Se in tri-*n*-octylphosphine (TOP−Se) was first prepared in a nitrogen-filled glove box by dissolving 0.395 g of elemental Se in 5 mL of TOP.

Bi Nanocrystals. Bi nanocrystals were prepared under a nitrogen atmosphere on a Schlenk line as described previously.[40] Bi(III) 2-ethylhexanoate was reduced at room temperature in a mixture of TOP and dioctylether with $NaBH_4$ in ethylenediamine. In one reaction flask, 0.1 mL of Bi(III) 2-ethylhexanoate and 0.15 mL of TOP were added to 11 mL of dioctylether and stirred at room temperature for 15 min. In a separate reaction flask, 30 mg of $NaBH_4$ was dissolved in 3.4 mL of ethylenediamine by heating to 45 °C and stirring for 15 min. This $NaBH_4$-reducing solution is then cooled to room temperature and rapidly injected into the Bi-(III) 2-ethylhexanoate/TOP/dioctylether solution. Over the course of minutes, the reaction mixture changes from a milky white to black color. The reaction mixture is removed from the Schlenk line after stirring for 30 min. The Bi nanocrystals are isolated by precipitation with ∼5 mL ethanol and then centrifugation at 8000 rpm for 5 min. The supernatant is discarded, and the Bi nanocrystals are stored in a nitrogen-filled glove box.

ZnSe Nanowire Synthesis in TOA. A four-neck reaction flask was attached to a Schlenk line and charged with 3 mL of TOA and either 11.7 or 23.4 mg of ZnO, depending on the desired Bi/Zn mole ratio of either 1:20 or 1:40, respectively. The TOA/ZnO mixture was dried and degassed by heating the reaction flask to 100 °C under vacuum for 1 h. The reaction flask was backfilled with nitrogen, and then either 200 μL (Bi/Zn=1:20) or 370 μL (Bi/Zn=1:40) of OA was added. This mixture was stirred for an additional 30 min under vacuum and then backfilled with nitrogen and heated to 350 °C. After approximately 20 min of stirring at 350 °C, the solution changed from milky to clear as a soluble OA−Zn complex formed. Once the hot (350 °C) TOA/ZnO/OA mixture became clear, a solution of 1.5 mg of Bi nanocrystals, 144 μL of 1 M TOP−Se, and 360 μL of toluene (for a Bi/Zn mole ration of 1:20) prepared in the glovebox was rapidly injected by syringe into the reaction flask. Alternatively, a solution of 1.5 mg of Bi nanocrystals, 287 μL of TOP−Se, and 217 μL of toluene can be injected for a Bi/Zn ratio of 1:40. The temperature drops by ∼10 °C. When the mixture returns to 350 °C, it is stirred for an additional 5 min, and then the reaction flask is removed from the heating mantle and allowed to cool to ∼60 °C.

ZnSe Nanowire Synthesis in TOPO. A four-neck reaction flask was attached to a Schlenk line and charged with 3 g of TOPO and 11.7 mg of ZnO. The TOPO/ZnO mixture was heated to 100 °C and held under vacuum for 1 h. The reaction flask was backfilled with nitrogen, and 200 μL of OA was added. The TOPO/ZnO/OA mixture was heated to 100 °C, held under vacuum for 30 min, and then backfilled with nitrogen and heated to 350 °C. After approximately 20 min of stirring at 350 °C, the TOPO/ZnO/OA mixture changed from milky to clear. A reagent solution of 1.5 mg of Bi nanocrystals, 144 μL of TOP−Se, and 360 μL of toluene (for a Bi/Zn mole ratio of 1:20) was prepared in the glovebox. Once the hot (350 °C) TOPO/ZnO/OA mixture was clear, this Se reagent solution was injected by syringe into the reaction flask. The temperature drops by ∼10 °C. The mixture is stirred for another 5 min after returning to 350 °C and then removed from the heating mantle and allowed to cool to ∼60 °C.

Nanowire Purification. A volume of 10 mL of toluene was added to the reaction flask after it had cooled to ∼60 °C. The reaction product was light green in color. The nanowire product was centrifuged at 8000 rpm for 10 min, and then the supernatant was discarded. The precipitate was redispersed in chloroform, reprecipitated with ethanol, and centrifuged again at 8000 rpm for 10 min. The supernatant was discarded. The reactions give a relatively high yield of nanowires. For example, in one TOA reaction, ∼27% of the ZnSe reactant was converted to the final isolated nanowire product.

Materials Characterization. Purified nanowires were characterized by scanning electron microscopy (SEM), transmission electron microscopy (TEM), energy dispersive X-ray spectroscopy (EDS), and X-ray diffraction (XRD). SEM images were obtained from nanowires on glassy-carbon substrates using a LEO 1530 field emission gun SEM operating at 3 kV accelerating voltage. TEM

(21) Chan, S. K.; Liu, N.; Cai, Y.; Wang, N.; Wong, G. K. L.; Sou, I. K. *J. Electron. Mater.* **2006**, *35*, 1246−1250.
(22) Xia, D.-Y.; Dai, L.; Xu, W.-J.; You, L.-P.; Zhang, B.-R.; Ran, G.-Z.; Qin, G.-G. *Chin. Phys. Lett.* **2006**, *23*, 1317−1320.
(23) Li, Q.; Gong, X.; Wang, C.; Wang, J.; Ip, K.; Hark, S. *Adv. Mater.* **2004**, *16*, 1436−1440.
(24) Colli, A.; Hofmann, S.; Ferrari, A. C.; Ducati, C.; Martelli, F.; Rubini, S.; Cabrini, S.; Franciosi, A.; Robertson, J. *Appl. Phys. Lett.* **2005**, *86*, 153103/1−153103/3.
(25) Chan, S. K.; Cai, Y.; Wang, N.; Sou, I. K. *Appl. Phys. Lett.* **2006**, *88*, 013108/1−013108/3.
(26) Zhang, X.; Liu, Z.; Li, Q.; Leung, Y.; Ip, K.; Hark, S. *Adv. Mater.* **2005**, *17*, 1405−1410.
(27) Zhang, X. T.; Liu, Z.; Ip, K. M.; Leung, Y. P.; Li, Q.; Hark, S. K. *J. Appl. Phys.* **2004**, *95*, 5752−5755.
(28) Xiang, B.; Zhang, H. Z.; Li, G. H.; Yang, F. H.; Su, F. H.; Wang, R. M.; Xu, J.; Lu, G. W.; Sun, X. C.; Zhao, Q.; Yu, D. P. *Appl. Phys. Lett.* **2003**, *82*, 3330−3332.
(29) Solanki, R.; Huo, J.; Freeouf, J. L.; Miner, B. *Appl. Phys. Lett.* **2002**, *81*, 3864−3866.
(30) Duan, X.; Lieber, C. M. *Adv. Mater.* **2000**, *12*, 298−302.
(31) Ye, C.; Fang, X.; Wang, Y.; Yan, P.; Zhao, J.; Zhang, L. *Appl. Phys. A: Mater. Sci. Process.* **2004**, *79*, 113−115.
(32) Zhu, Y.-C.; Bando, Y. *Chem. Phys. Lett.* **2003**, *377*, 367−370.
(33) Xiong, S.; Shen, J.; Xie, Q.; Gao, Y.; Tang, Q.; Qian, Y. *Adv. Funct. Mater.* **2005**, *15*, 1787−1792.
(34) Panda, A. B.; Acharya, S.; Efrima, S. *Adv. Mater.* **2005**, *17*, 2471−2474.
(35) Dong, Y.; Peng, Q.; Li, Y. *Inorg. Chem. Commun.* **2004**, *7*, 370−373.
(36) Panda, A. B.; Glaspell, G.; El-Shall, M. S. *J. Am. Chem. Soc.* **2006**, *128*, 2790−2791.
(37) Dong, A.; Wang, F.; Daulton, T. L.; Buhro, W. E. *Nano Lett.* **2007**, *7*, 1308−1313.
(38) Zhai, T.; Zhong, H.; Gu, Z.; Peng, A.; Fu, H.; Ma, Y.; Li, Y.; Yao, J. *J. Phys. Chem. C* **2007**, *111*, 2980−2986.
(39) Hu, J.; Bando, Y.; Golberg, D. *Small* **2005**, *1*, 95−99.
(40) Fanfair, D. D.; Korgel, B. A. *Cryst. Growth Des.* **2005**, *5*, 1971−1976.

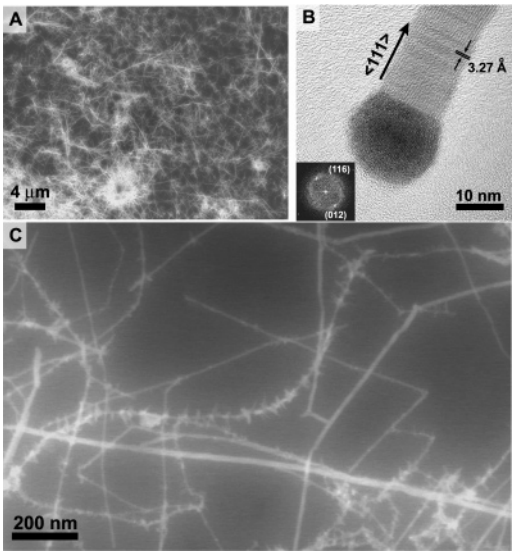

Figure 1. (A and C) SEM and (B) TEM images of Bi-seeded ZnSe nanowires produced in TOA with a Bi/Zn mole ratio of 1:40. The fast Fourier transform-produced image in the inset in B is of the seed nanocrystal at the nanowire end: the bright spots index to the (012) and (116) planes of rhombohedral Bi (JCPDS Card 44-1246). In C, several nanowires are observed to have short branches along their length.

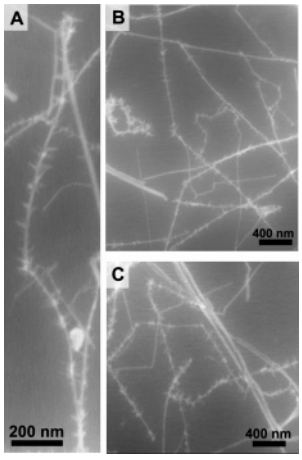

Figure 2. (A−C) SEM images of Bi-seeded ZnSe nanowires produced in TOA with a Bi/Zn mole ratio of 1:40.

images were obtained from nanowires on 200-mesh lacey carbon-coated Cu grids (Electron Microscopy Sciences) imaged using a JEOL 2010F field emission gun electron microscope operating at 200 kV accelerating voltage. EDS data was acquired using an Oxford INCA spectrometer on the JEOL 2010F TEM. XRD data was acquired from ∼0.5 mg of nanowires deposited on a quartz slide using a Bruker-Nonius D8 Avance θ-2θ powder diffractometer with Cu Kα radiation (λ = 1.5418 Å) and collecting with a scintillation detector for 16 h with an incremental angle of 0.02° at a scan rate of 12°/min.

Results

ZnSe Nanowires Synthesized in TOA. Figures 1 and 2 show SEM and TEM images of ZnSe nanowires obtained from reactions in TOA. The nanowires have high aspect ratios (>100), with lengths ranging from 1 to 10 μm and diameters ranging from 10 to 40 nm. XRD and EDS (Figure 3) confirmed that the nanowires are ZnSe. The *d*-spacing between lattice planes perpendicular to the growth direction determined by high-resolution TEM was 3.27 Å, which

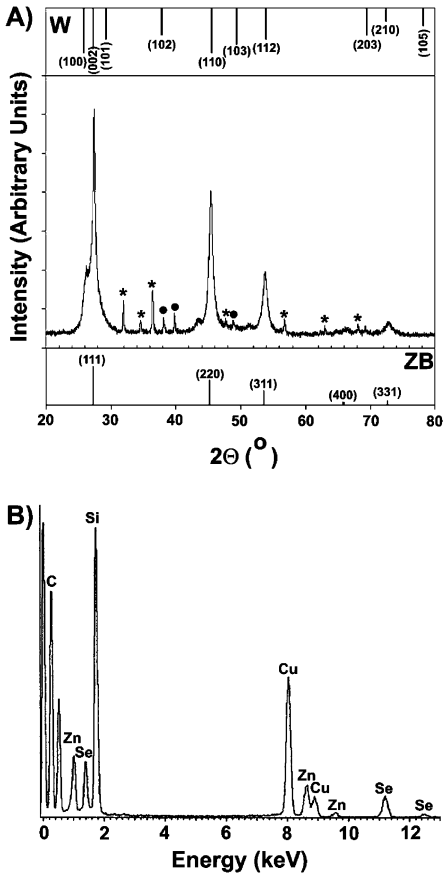

Figure 3. (A) XRD and (B) EDS graphs of Bi-seeded ZnSe nanowires grown in TOA with a Bi/Zn mole ratio of 1:40. Peaks in A labeled with "∗" and "●" index to Bi and zincite (hexagonal ZnO), respectively. As confirmed by TEM and EDS, the nanowires are composed of ZnSe, and ZnO is a reaction byproduct. "**W**" and "**ZB**" in A correspond to wurtzite (JCPDS: 15-0105) and zinc blende (JCPDS: 37-1463) ZnSe, respectively.

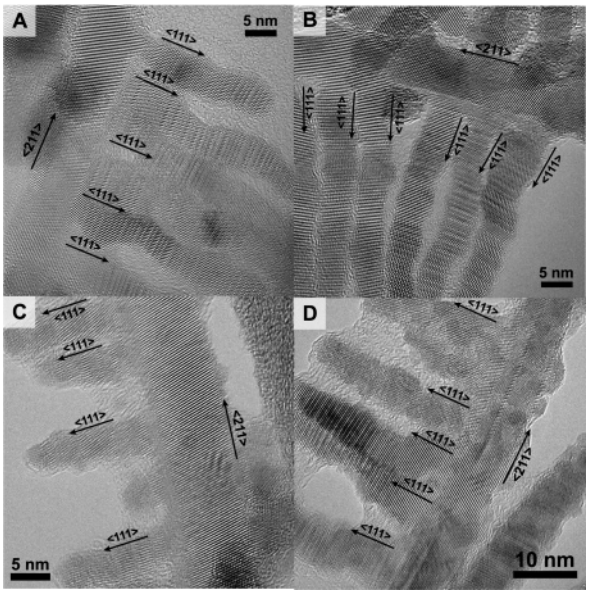

Figure 4. (A−D) TEM images of Bi-seeded ZnSe nanowires produced in TOA with Bi/Zn mole ratios of (A and D) 1:20 and (B and C) 1:40. The nanowire growth direction is <211>, and the branches grow in the <111> direction, perpendicular to the nanowire trunk.

corresponds to the (111) d spacing of sphalerite (cubic) ZnSe (3.2729 Å). Figure 1B shows an example of a ZnSe nanowire with zinc blende crystal structure, a <111> growth direction, and a Bi seed particle at its tip. TEM analysis of 75

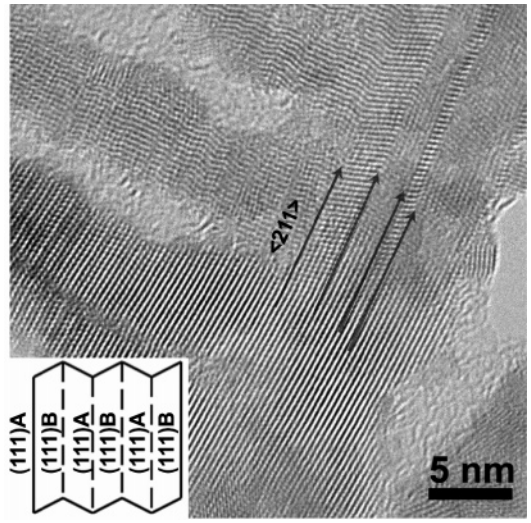

Figure 5. <211>-oriented ZnSe nanowire with {111} twin planes in its core, as indicated by arrows. The {111} twins in the branches extend parallel to the multiple {111} branches in the nanowire core. The inset illustrates a series of (111) twin planes (dashed lines).

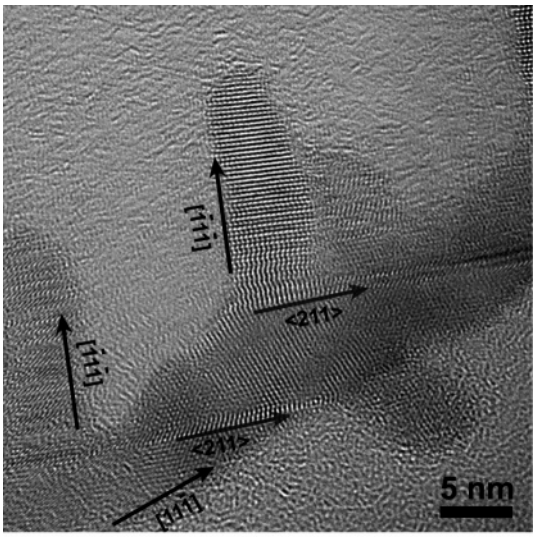

Figure 6. TEM image of <111>-oriented Bi-seeded ZnSe nanowire produced in TOA using a 1:20 molar ratio of Bi/Zn. This nanowire is viewed down the [011] zone axis. Arrows indicate (111) twin planes with a <211> direction.

nanowires showed that 57% of the nanowires have a <111> growth direction and 43% of the nanowires have a <211> growth direction. Nanowires were not observed in reactions in which Bi nanocrystals were not added to the reactions.

Further inspection of the SEM images, as in Figures 1C and 2, reveals that the ZnSe nanowires synthesized in TOA have a large number of short branches along their length. TEM imaging, as in Figures 4−6, shows that the branches grow from 10 to 35 nm in length off the nanowire surface and range from 5 to 6 nm in diameter. All of the branches have crystallized in the <111> direction and are epitaxially interfaced with the nanowire. The branches are also heavily twinned, with {111} twins bisecting their <111> growth direction. Furthermore, most of the branches grow perpendicular to the nanowire growth direction. This branch orientation is not possible for nanowires with <111> growth direction, and the vast majority of nanowires with sidewall branching have grown in the <211> direction, which is

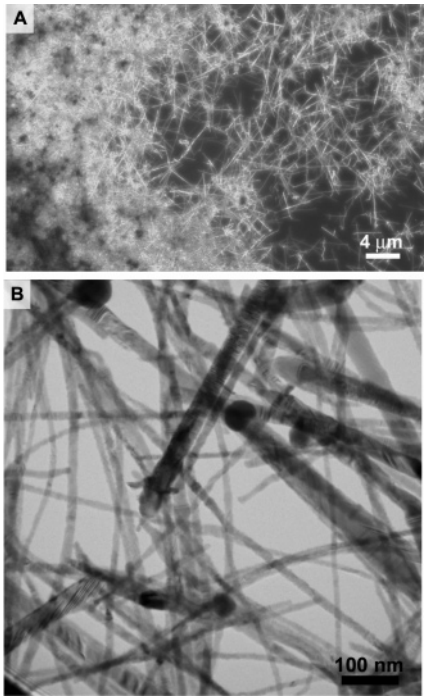

Figure 7. (A) SEM and (B) TEM images of Bi-seeded ZnSe nanowires grown in TOPO as the solvent using a 1:20 molar ratio of Bi/Zn.

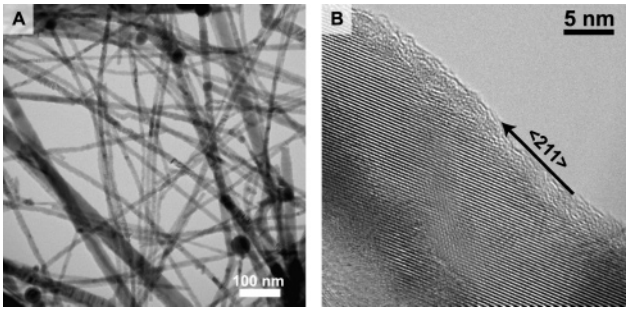

Figure 8. (A and B) TEM images of Bi-seeded ZnSe nanowires produced in TOPO using a Bi/Zn mole ratio of 1:20.

oriented at 90° with respect to the <111> crystallographic direction. Although the <211> growth direction is less energetically favorable than the more common <111> growth direction for nanowires with zinc blende crystal structure (as observed in GaAs[41] and GaP[42,43] nanowires, for example), {111} twins extending down the nanowire length can promote the <211>-oriented growth of zinc blende nanowires. For instance, this kind of {111} twin plane-directed <211> growth has been observed for gold nanocrystal-seeded Si and Ge nanowires.[44,45] (The diamond cubic and zinc blende crystal structures are isostructural.) In fact, lamellar {111} twins running down the length of ZnSe nanowires with <211> growth direction are commonly

(41) Davidson, F. M., III; Schricker, A. D.; Wiacek, R. J.; Korgel, B. A. *Adv. Mater.* **2004**, *16*, 646−649.
(42) Davidson, F. M., III; Wiacek, R.; Korgel, B. A. *Chem. Mater.* **2005**, *17*, 230−233.
(43) Johansson, J.; Karlsson, L. S.; Svensson, C. P. T.; Martensson, T.; Wacaser, B. A.; Deppert, K.; Samuelson, L.; Seifert, W. *Nat. Mater.* **2006**, *5*, 574−580.
(44) Korgel, B. A.; Lee, D. C.; Hanrath, T.; Yacaman, M. J.; Thesen, A.; Matijevic, M.; Kilaas, R.; Kisielowski, C.; Diebold, A. C. *IEEE Trans. Semicond. Manuf.* **2006**, *19*, 391−396.
(45) Davidson, F. M., III; Lee, D. C.; Fanfair, D. D.; Korgel, B. A. *J. Phys. Chem. C* **2007**, *111*, 2929−2935.

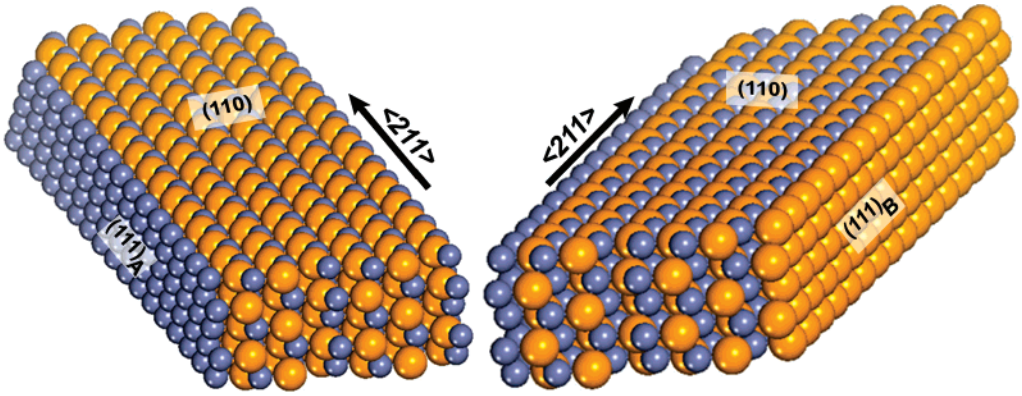

Figure 9. Crystallographic model of a <211>-oriented nanowire. The blue and golden spheres represent Zn and Se, respectively.

observed, as in Figures 4D and 5. It should be noted that in many TEM images of <211>-oriented nanowires, {111} twin planes are not observed because the nanowire must be imaged precisely down the <110> zone axis for them to be visible. In only a few rare cases, as in Figure 6, are the branches oriented at an angle to the nanowire growth direction. But even in this case, it appears that {111} twins expose reactive surfaces that lead to sidewall branch growth.

The large concentration of {111} twins observed in the nanowires and their branches by TEM is consistent with the XRD data (Figure 3A). The XRD patterns of ZnSe nanowires appear to show a mixture of hexagonal (wurtzite) and cubic (zinc blende) phases—for example, there is a first-order diffraction peak that can be indexed to the hexagonal (100) planes of wurtzite ZnSe, which does not have a corresponding d spacing in zinc blende ZnSe; however, a large concentration of twins in the sample can also give rise to such diffraction patterns.[46] A {111} twin occurs by a 60° twist of the crystal lattice along the [111] direction.[47] This twist allows all of the bonds in the crystal to be satisfied and thus requires very little energy to occur. As such, twins are common extended defects in zinc blende crystals, disrupting the ABCABC layering of close-packed planes and giving rise to a reflection in symmetry, as in ABCAB/ACBA. The layer stacking at the twin gives the appearance (at least on an atomic scale) of the characteristic ABABAB stacking of the wurtzite phase. If a cubic crystal has enough {111} twins, XRD data can give the appearance that the sample has a mixture of cubic and hexagonal crystal structure, as Hamada et al.[46] have shown. Lamellar {111} twinning has been found to commonly occur in nanowires with zinc blende crystal structure, including GaAs,[41] GaP,[42,43] ZnSe,[23] ZnS,[48] and InAs.[49] Careful examination of many high-resolution TEM images of the ZnSe nanowires indicates that they are predominantly zinc blende with a large concentration of {111} twins. The ZnSe nanowire in Figure 1B, for example, exhibits a <111> growth direction with a large concentration of lamellar {111} twins.

ZnSe Nanowires Synthesized in TOPO. Nanowires grown in TOPO did not show branching. Figures 7 and 8 show TEM and SEM images of ZnSe nanowires synthesized in TOPO. There is no branching from these nanowires. This result is consistent with a recent ZnSe nanowire synthesis from Buhro's group,[37] in which ZnSe nanowires grown in TOPO did not exhibit branching. The predominant growth direction of these nanowires was <111>, and <111>-oriented branches cannot grow perpendicular to their growth direction; however, even nanowires observed with a <211> growth direction (synthesized in TOPO), as in Figure 8B, did not exhibit secondary branch growth from their sidewall surfaces.

Discussion

Crystallographic Model for ZnSe Nanowire Branched Growth and the Role of the Solvent. TEM imaging of many ZnSe nanowires grown in TOA revealed that the branches extend predominantly from only one side of the nanowire. This anisotropic branched growth appears to result from three related factors: (1) Branches crystallize epitaxially from {111} sidewall facets of <211>-oriented nanowires; (2) the {111} surfaces of ZnSe are polar and terminate predominantly with either Zn (the $(111)_A$ surface) or Se (the $(111)_B$ surface), and to maintain charge neutrality across the nanowire, one side of the wire exposes a $(111)_A$ surface and the other side exposes a $(111)_B$ surface; and (3) TOA bonds more weakly to the Zn-terminated surface than to the Se-terminated surface, allowing branching to occur exclusively from the $(111)_A$ surfaces. Figure 9 shows a crystallographic model of a ZnSe nanowire with a <211> growth direction. The <211> growth direction is expected to result in square sidewall faceting that exposes two opposing {110} and {111} surfaces.[50] Since the branches crystallize in the <111> direction and epitaxially interface with the nanowire sidewall surface, the branches must be growing exclusively from the {111} sidewall facets. TOA is a tertiary amine that forms dative bonds with Zn and Se through its lone pair of electrons on the nitrogen atom. The N−Se bond energy (381 kJ mol^{-1})[51] is stronger than the N−Zn bond energy,[52] and

(46) Hamada, E.; Cho, W.-S.; Takayanagi, K. *Philos. Mag. A* **1998**, *77*, 1301−1308.
(47) Korgel, B. A. *Nat. Mater.* **2006**, *5*, 521−522.
(48) Hao, Y.; Meng, G.; Wang, Z. L.; Ye, C.; Zhang, L. *Nano Lett.* **2006**, *6*, 1650−1655.
(49) Xu, X.; Wei, W.; Qiu, X.; Yu, K.; Yu, R.; Si, S.; Xu, G.; Huang, W.; Peng, B. *Nanotechnology* **2006**, *17*, 3416−3420.
(50) Hanrath, T.; Korgel, B. A. *Small* **2005**, *1*, 717−721.
(51) Speight, J. G. *Lange's Handbook of Chemistry*, 16th ed.; McGraw-Hill: New York, 2005.

therefore, sidewall nucleation and branch growth is more likely on the Zn-terminated $(111)_A$ sidewall surface than on the Se-terminated $(111)_B$ surface.

TOPO bonds to Zn and Se dangling bonds via its two lone pairs of electrons on the O atom. O forms a relatively strong bond with both Zn and Se, as in the O−Zn (284.1 kJ mol^{-1})[51] and O−Se (423 kJ mol^{-1}) bonds,[51] whereas N bonds strongly to Se, as a N−Se bond (381 kJ mol^{-1}),[51] but not to Zn.[52] Therefore, TOPO better passivates the sidewall surfaces of the nanowires and inhibits branching by adsorbing onto the nanowire surface.

Conclusions

ZnSe nanowires grown by the SLS mechanism using Bi nanocrystals as seeds exhibited a significant amount of secondary nucleation and growth on the nanowire sidewall surfaces when TOA was used as a solvent. In contrast, branching was not observed when TOPO was used as a solvent. TOPO is a stronger passivating agent on the nanowire surface. Interestingly, the sidewall branches grow predominantly from only one side of the nanowires, most likely due to weaker bonding between TOA and the Zn-terminated $(111)_A$ sidewall surfaces than the opposing Se-terminated $(111)_B$ sidewall surfaces. {111} twins are also intimately associated with sidewall branched growth. Lamellar {111} twins extending down the lengths of the nanowires enable the <211> growth direction that provides the structural basis for perpendicular <111> branch growth. The branches themselves exhibit a very high concentration of {111} twins.

It is worth noting that the branched growth off the surfaces of these ZnSe nanowires probably relates to the branched growth observed in semiconductor nanocrystals precipitated in hot coordinating solvents, as in tetrapods, bipods, tripods, and "arrowheads" of a variety of materials, including CdS,[53,54] CdSe,[55−57] CdTe,[58−61] ZnSe,[62,63] and PbSe.[64] In these systems, the bonding between the coordinating solvent and the semiconductor surface strongly influences branching. For branching to occur, the ligands must be strong enough to control nanocrystal growth, but weak enough to allow secondary nucleation. Twinning is probably central to nanocrystal branching as well, which has indeed been recently proposed by Manna and co-workers[65] for CdTe tetrapod formation and Bando and co-workers[66] for ZnSe tetrapods. The relative bond strengths between the solvent and the semiconductor surface and the likelihood of twinning in the semiconductor are both (probably related) influential factors in the branched growth of semiconductor nanocrystals and nanowires. Understanding how to control these factors will lead to the general availability of a very interesting class of nanomaterials with extremely high surface area-to-volume ratios and directional electronic and optical properties.

Acknowledgment. We thank Doh C. Lee and Hsing-Yu Tuan for insightful discussions. We also thank Dr. J. P. Zhou for TEM assistance. We acknowledge the National Science Foundation through their STC program (Grant No. CHE-9876674), the Office of Naval Research (N00014-05-1-0857), DARPA through the Advanced Processing and Prototyping Center (HR0011-06-1-0005), and the Robert A. Welch Foundation for their financial support for this work.

CM071440T

(52) To the best of our knowledge, the N−Zn bond energy has not been measured; however, it should be weaker than the N−Se, O−Zn, and O−Se bond energies: Boldyrev, A. I.; Simons, J. *Mol. Phys.* **1997**, *92*, 365−379.

(53) Jun, Y.-w.; Lee, S.-M.; Kang, N.-J.; Cheon, J. *J. Am. Chem. Soc.* **2001**, *123*, 5150−5151.
(54) Chen, M.; Xie, Y.; Lu, J.; Xiong, Y.; Zhang, S.; Qian, Y.; Liu, X. *J. Mater. Chem.* **2002**, *12*, 748−753.
(55) Kanaras, A. G.; Soennichsen, C.; Liu, H.; Alivisatos, A. P. *Nano Lett.* **2005**, *5*, 2164−2167.
(56) Manna, L.; Scher, E. C.; Alivisatos, A. P. *J. Am. Chem. Soc.* **2000**, *122*, 12700−12706.
(57) Peng, Z. A.; Peng, X. *J. Am. Chem. Soc.* **2002**, *124*, 3343−3353.
(58) Manna, L.; Milliron, D. J.; Meisel, A.; Scher, E. C.; Alivisatos, A. P. *Nat. Mater.* **2003**, *2*, 382−385.
(59) Yu, W. W.; Wang, Y. A.; Peng, X. *Chem. Mater.* **2003**, *15*, 4300−4308.
(60) Bunge, S. D.; Krueger, K. M.; Boyle, T. J.; Rodriguez, M. A.; Headley, T. J.; Colvin, V. L. *J. Mater. Chem.* **2003**, *13*, 1705−1709.
(61) Peng, Z. A.; Peng, X. *J. Am. Chem. Soc.* **2001**, *123*, 183−184.
(62) Cozzoli, P. D.; Manna, L.; Curri, M. L.; Kudera, S.; Giannini, C.; Striccoli, M.; Agostiano, A. *Chem. Mater.* **2005**, *17*, 1296−1306.
(63) Li, L. S.; Pradhan, N.; Wang, Y.; Peng, X. *Nano Lett.* **2004**, *4*, 2261−2264.
(64) Shi, W.; Sahoo, Y.; Zeng, H.; Ding, Y.; Swihart, M. T.; Prasad, P. N. *Adv. Mater.* **2006**, *18*, 1889−1894.
(65) Carbone, L.; Kudera, S.; Carlino, E.; Parak, W. J.; Giannini, C.; Cingolani, R.; Manna, L. *J. Am. Chem. Soc.* **2006**, *128*, 748−755.
(66) Hu, J.; Bando, Y.; Golberg, D. *Small* **2005**, *1*, 95−99.